Revista de la Academia Colombiana de Ciencias Exactas, Físicas y Naturales. 2026
doi: https://doi.org/10.18257/raccefyn.4169

Physical Sciences

Original article

Neuromorphic computing with quantum materials: From Mott insulators to brain-inspired devices

Computación neuromórfica con materiales cuánticos: de los aislantes de Mott a los dispositivos bioinspirados

Juan Gabriel Ramírez[1,*], Pedro Prieto[2], María E. Gómez[2], Ivan K. Schuller[3]

[1] Departamento de Física, Universidad de los Andes, Bogotá, Colombia
[2] Departamento de Física, Universidad del Valle, Cali, Colombia
[3] Physics Department, University of California San Diego, La Jolla, USA

Abstract

The escalating energy demands of modern artificial intelligence have exposed fundamental limitations in conventional computing architectures. Neuromorphic computing, which seeks to emulate the brain's massively parallel and energy-efficient information processing, offers a compelling alternative, but its realization requires materials that naturally exhibit nonlinear, multi-state, and adaptive behavior characteristic of biological neurons and synapses. This review argues that strongly correlated electron materials, particularly Mott insulators, provide exactly this physical substrate. We present the essential physics of metal-insulator transitions in vanadium oxides (VO_2, V_2O_3) and perovskite manganites in an accessible manner and describe how their switching behaviors map onto neuromorphic primitives: the neuristor (artificial neuron) and the synaptor (artificial synapse). The review draws extensively on the authors' experimental work: direct imaging of nanotextured phase coexistence in V_2O_3; an MIT Fingerprinting approach to engineer multi-state resistive switching in VO_2; the demonstration of subthreshold firing in Mott nanodevices; and electrically controlled multi-state analog memory in phase-separated manganites. The review concludes by identifying the main challenges and the most promising directions to translate these laboratory demonstrations into practical brain-inspired computing systems.

Keywords: Neuromorphic computing; Mott insulator; metal-insulator transition; vanadium dioxide; neuristor; synaptor.

Resumen

Las crecientes demandas energéticas de la inteligencia artificial moderna han expuesto las limitaciones fundamentales de las arquitecturas de cómputo convencionales. La computación neuromórfica, que busca emular el procesamiento de información altamente paralelo y eficiente del cerebro, ofrece una alternativa convincente cuya realización ha requerido materiales que exhiban de forma natural el comportamiento no lineal, multiestado y adaptativo que caracteriza a las neuronas y las sinapsis biológicas. En esta revisión se plantea que los materiales con electrones fuertemente correlacionados, en particular los aislantes de Mott, proporcionan exactamente ese sustrato físico. Se presenta de manera accesible la física esencial de las transiciones metal-aislante en óxidos de vanadio (VO_2, V_2O_3) y manganitas de perovskita, y se describe cómo su comportamiento de conmutación se traduce en primitivas neuromórficas: el neuristor (neurona artificial) y el sinaptor (sinapsis artificial). La revisión se apoya ampliamente en el trabajo experimental de los autores: la visualización directa de la coexistencia de fases nanotexturadas en V_2O_3; la técnica de huellas del MIT para la ingeniería de la conmutación resistiva multiestado en VO_2; la demostración del disparo subumbral en nanodispositivos de Mott, y la memoria analógica multiestado controlada eléctricamente en manganitas con separación de fases. Se concluye con la presentación de los principales retos y las perspectivas más prometedoras para llevar estas demostraciones de laboratorio a su aplicación en sistemas prácticos de cómputo bioinspirado.

Palabras clave: computación neuromórfica; aislante de Mott; transición metal-aislante; dióxido de vanadio; neuristor; sinaptor.

Citation: Ramírez JG, et al. Neuromorphic computing with quantum materials: From Mott insulators to brain-inspired devices. Revista de la Academia Colombiana de Ciencias Exactas, Físicas y Naturales. 2026 Sep 23. doi: https://doi.org/10.18257/raccefyn.4169

Editor: Jairo Roa Rojas

***Corresponding author:**
Juan Gabriel Ramírez;
jgramirez@uniandes.edu.co

Received: July 16, 2026
Accepted: August 19, 2026
Published on line: September 23, 2026

This is an open access article distributed under the terms of the Creative Commons Attribution License.

Revista de la Academia Colombiana de Ciencias Exactas, Físicas y Naturales. 2026
doi: https://doi.org/10.18257/raccefyn.4169

Introduction

Modern computing faces a rapidly growing energy demand. Training a single large artificial intelligence (AI) model currently can consume more electricity than five average households use in an entire year (**Cao *et al*.**, 2022; del **Valle *et al*.**, 2018). As AI applications spread across medical diagnostics, autonomous vehicles, climate modeling, and real-time language processing, the energy footprint of computing is on track to become one of the dominant sources of global electricity demand. The fundamental cause is architecture. The conventional *von Neumann* paradigm, in which a central processor fetches data from a physically separate memory through a shared bus, was not designed for the massive data-parallel computations that underlie modern deep learning. Each arithmetic operation requires a costly round-trip between processor and memory— the so-called "memory-bandwidth bottleneck." See Fig. 1. Current AI accelerators built from billions of silicon transistors alleviate this bottleneck through brute-force hardware parallelism, but at the cost of kilowatts of power and enormous chip area.

The human brain performs the same kinds of pattern recognition and sensory processing as state-of-the-art AI, yet it consumes only approximately 20 watts—comparable to a dim incandescent bulb. An NVIDIA H100 GPU contains a similar number of silicon transistors ($\sim 80 \times 10^9$) yet draws 700 W at peak load—a 35-fold power penalty at comparable unit count (Fig. 1c). Remarkably, this efficiency gap extends across all of biology: from the fruit fly ($\sim$135 000 neurons, 27 µW) to the elephant ($\sim 257 \times 10^9$ neurons, $\sim$69 W), the metabolic power of biological brains—inferred from oxygen consumption, not measured electrically—scales with a characteristic energy budget near 0.22 nW per neuron (**Attwell** & **Laughlin**, 2001), a rough but surprisingly stable biological scaling law spanning seven orders of magnitude in neuron count (with roughly two-fold scatter across species; the elephant data point lies somewhat above the trend, consistent with its larger average neuron size). This extraordinary efficiency arises from a fundamentally different computational architecture: memory and computation are co-located. Each synapse both *stores* a learned connection weight and *participates* in the computation when a signal flows through it. There is no central processor and no memory bus. Instead, roughly 86 billion neurons each receive thousands of synaptic inputs, integrate them continuously over time, and emit brief electrical pulses—"spikes"—whenever a threshold is exceeded, then reset. Information is encoded in the timing and frequency of spikes rather than in precise binary voltage levels, making the system inherently robust to noise. **Mead** (1989) captured the key insight decades ago: "the nervous system of even a very simple animal contains computing paradigms that are orders of magnitude more effective than are those found in systems made by humans."

Neuromorphic computing seeks to translate these biological principles into hardware. The field has produced dedicated chips such as Intel's Loihi (**Davies *et al*.**, 2018) and IBM's TrueNorth (**Merolla *et al*.**, 2014), which implement brain-inspired architectures in conventional CMOS technology and demonstrate significant energy savings for specific tasks. Yet a deeper limitation persists inasmuch as silicon transistors are binary, deterministic switches, and elaborate circuits are required to emulate the rich, continuous, and history-dependent dynamics of biological neurons and synapses. The missing ingredient is a class of materials that naturally and efficiently exhibits nonlinear switching, multi-state memory, and adaptive behavior (del **Valle *et al*.**, 2018).

This review argues that strongly correlated electron materials—particularly Mott insulators (**Laad** & **Craco**, 2024)—provide exactly this missing ingredient. These quantum materials undergo dramatic metal-insulator transitions (MIT) triggered by temperature, electric field, light, strain, or magnetic field, switching their electrical resistance by several orders of magnitude in a highly nonlinear fashion. This natural switching behavior maps directly onto the functions required for neuromorphic primitives. This review focuses on establishing these physical primitives at the single-device level; scaling them into networks trained

under realistic workloads is discussed as a research direction in the Challenges and Future Directions section.

We present the essential physics of Mott materials in an accessible manner and organize the experimental discussion around four results, presented in order from material physics to device functionality: (i) direct near-field imaging of nanotextured phase coexistence in V_2O_3, (ii) MIT Fingerprinting for rational multi-state device engineering, (iii) subthreshold firing in Mott nanodevices, and (iv) multi-state analog memory in phase-separated manganites and multiferroic oxides.

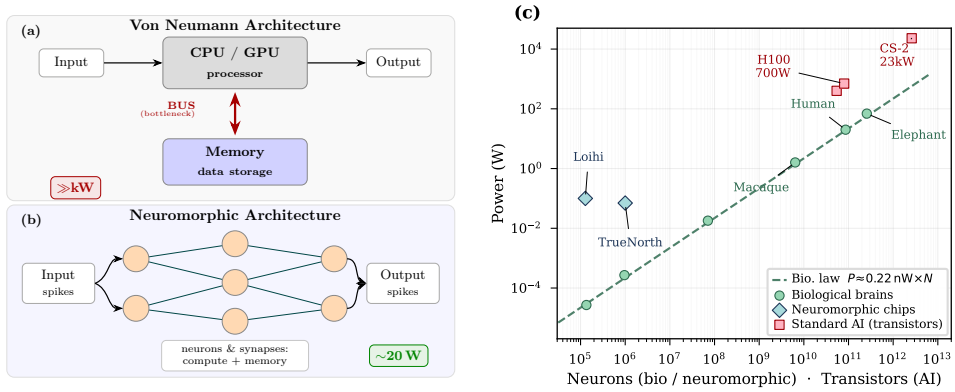

Figure 1. The von Neumann bottleneck and the neuromorphic alternative. (a) Von Neumann architecture: processor and memory separated by a shared bus. (b) Neuromorphic architecture: compute and memory co-located at each node. (c) Power vs. number of processing units for biological brains (circles; neuron counts from **Herculano-Houzel** (2009)), neuromorphic chips—TrueNorth (**Merolla *et al*.**, 2014), Loihi (**Davies *et al*.**, 2018) (diamonds)—and AI accelerators (squares), including an NVIDIA H100 GPU and the Cerebras CS-2 (**Lie**, 2021). Dashed line: biological metabolic scaling law, $P \approx 0.22\,\mathrm{nW} \times N$ (**Attwell** & **Laughlin**, 2001), labeled "Bio. law" in the legend.

The Brain's Computing Principles and What We Need to Emulate

To understand why Mott insulators are promising for neuromorphic hardware, it is useful to be precise about what needs to be emulated. A biological neural network consists of two functional elements: *neurons* and *synapses*.

Neurons are the computing units. When a neuron receives enough electrical excitation through its dendrites, a membrane voltage rises; if it crosses a threshold, the neuron "fires" a brief action potential that travels along its axon to connected synapses. After firing, the membrane voltage resets and the neuron enters a refractory period. This behavior—integrate, fire, reset—is captured by the leaky-integrate-and-fire (LIF) model and is the most widely used abstraction for artificial neuron design. To emulate it in hardware, a material must exhibit *volatile*, threshold-based switching: the resistance drops abruptly when a stimulus exceeds a threshold and recovers spontaneously when the stimulus is removed.

Synapses are the memory elements. A synapse modulates the strength of the electrical signal between two neurons, and this strength—the *synaptic weight*—is modified by activity. "Neurons that fire together, wire together" summarizes the Hebbian learning rule: coincident pre- and post-synaptic activity strengthens the synapse, while anti-coincident activity weakens it. Emulating a synapse in hardware requires a material with *non-volatile*, multi-state resistance that can be incrementally modified by electrical pulses and retains its value when the stimulus is removed.

Revista de la Academia Colombiana de Ciencias Exactas, Físicas y Naturales. 2026
doi: https://doi.org/10.18257/raccefyn.4169

These two requirements—volatile threshold switching for neurons and non-volatile analog resistance modulation for synapses—define the materials challenge at the heart of neuromorphic computing (del **Valle** ***et al***., 2018). No single conventional material naturally satisfies both with high energy efficiency. Mott insulators, as described in the following sections, come remarkably close.

The Physics of Metal-Insulator Transitions

The Mott transition: an electron traffic jam

Most students of physics learn that a material with a half-filled electron band should be a metal. Yet there exists a large and fascinating class of transition-metal oxides—including vanadium and nickel compounds—that defy this prediction: despite their half-filled bands, they are electrical insulators. Sir Nevill Mott, winner of the 1977 Nobel Prize in Physics, first explained this paradox, and the phenomenon bears his name.

The key is *electron-electron Coulomb repulsion*. When two electrons try to occupy the same atomic site, they repel each other with an energy cost U. If this repulsion energy greatly exceeds the kinetic energy gain t from electron hopping between neighboring atoms (related to the bandwidth W), electrons prefer to stay localized on their own atoms to avoid the repulsion. The result is a *Mott insulator*: a material with a half-filled band that is insulating because of strong electron-electron interactions. A simple analogy is an electron traffic jam: the road (the band) is half full, but the vehicles (electrons) cannot move because they would collide with each other.

The ratio U/W governs whether a material is a Mott insulator. By changing temperature, pressure, chemical composition, or by applying an external field, one can tune U/W across a critical value and drive the system from insulating to metallic—a *Mott transition*. Many Mott insulators also have a structural component: the crystal lattice distorts as electrons localize or delocalize, coupling electronic and lattice degrees of freedom (**Goodenough**, 1971; **Imada**, **Fujimori**, & **Tokura**, 1998).

How a transition-metal oxide switches

The practical consequence of a Mott transition is a dramatic change in electrical resistance, often spanning four to six orders of magnitude. In vanadium dioxide (VO_2), this change occurs near 340 K (67°C)—very close to room temperature—making it particularly attractive for applications. Below the transition temperature, VO_2 is a monoclinic insulator with paired V-V dimers. Above it, the dimers break and the material becomes a metallic rutile phase (**Goodenough**, 1971). This insulator-to-metal transition can be triggered not only thermally but also by: an electric field or current (via Joule heating or carrier injection (**Valmianski** ***et al***., 2018)), by an ultrafast laser pulse (**Morrison** ***et al***., 2014; **Wang** ***et al***., 2017), or by epitaxial strain, which modifies the V-V dimerization and can even stabilize novel metallic phases (**McLeod** ***et al***., 2017).

This metal-insulator transition (MIT) and its physical manifestations are summarized schematically in Fig. 2. The transition is classically observed as a thermal hysteresis loop in resistance (R-T curve) under an external stimulus (see Fig. 2a). When an electric current is applied, the material switches from a high-resistance insulating state to a low-resistance metallic state, manifesting as a volatile threshold switching event or negative differential resistance (NDR) with discrete voltage drops in nanoscale devices (**Sharoni**, **Ramírez**, & **Schuller**, 2008; **Wang**, **Ramírez**, & **Schuller**, 2015) (see Fig. 2b). At the microscopic scale, the transition proceeds via the nucleation and growth of metallic domains coexisting within the insulating matrix (see Fig. 2c); the macroscopic resistance drop occurs once the metallic fraction crosses the percolation threshold ($p_c \approx 0.59$ for 2D site percolation on a square lattice; the exact value is geometry- and dimensionality-dependent in real films), as shown by the phase-fraction hysteresis curves in Fig. 2d.

This exceptional tunability—the ability to trigger the switch through temperature, electric field, light, or strain—is the key feature that makes vanadium oxides and related materials attractive for neuromorphic device design. The same underlying physics that causes a dramatic resistance change on heating can be exploited electrically to implement artificial neurons and synapses.

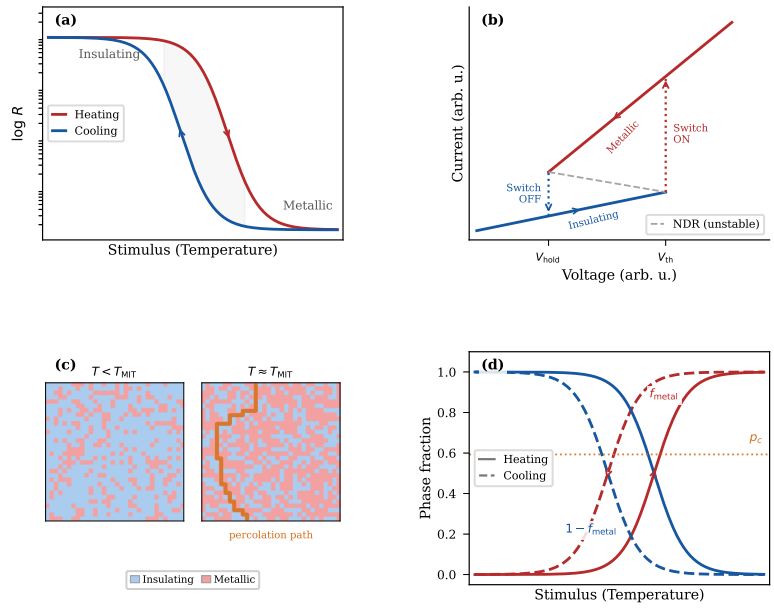

Figure 2. Physics of the metal-insulator transition. (a) Resistance hysteresis under a cyclic stimulus. (b) Volatile threshold I-V: switch-ON at V_{th}, switch-OFF at V_{hold}; dashed line is the NDR region. (c) 2D percolation simulation: isolated metallic nuclei below T_{MIT} (left) and a percolating cluster at $T \approx T_{\text{MIT}}$ (right). (d) Phase fractions vs. stimulus; dotted line marks p_c.

Key Material Systems

Vanadium dioxide (VO_2): the workhorse

VO_2 is the most intensively studied Mott-Peierls system for neuromorphic applications. Its near-room-temperature MIT is sharp (occurring over ∼5 K in thin films), accompanied by a large resistance change (∼4 orders of magnitude), and can be triggered reliably by electrical pulses. In VO_2, the transition is not purely electronic: in addition to Mott-type electron-electron correlations, a structural instability causes the crystal lattice to dimerize as electrons localize—the *Peierls mechanism* (**Goodenough**, 1971). While Peierls originally formulated this for one-dimensional chains, it applies here in three dimensions. Rather than competing, Mott and Peierls physics cooperate to stabilize the insulating state, classifying VO_2 as a hybrid *Mott-Peierls* system (**Weber *et al*.** 2012). The relative weight of each contribution is not settled, however: it remains an active area of research, with re-ported differences that depend on strain, doping level, sample quality, and the experimental timescale probed, so this hybrid classification should be read as an interpretive framework rather than a fixed quantitative split between the two mechanisms. This coupling enriches the switching behavior: both electronic and structural degrees of freedom respond to voltage, temperature, or optical stimuli.

When a thin-film VO_2 device is biased with a current pulse, local Joule heating drives the insulating region above the MIT temperature, creating a conductive metallic filament. Indeed, del **Valle *et al*.** (2021) used spatiotemporal imaging to map in real time the nucleation and growth of the metallic filament during voltage-induced switching; **Salev *et al*.**

Revista de la Academia Colombiana de Ciencias Exactas, Físicas y Naturales. 2026
doi: https://doi.org/10.18257/raccefyn.4169

(2024) resolved the distinct contributions of Joule heating and direct electric-field effects to filament formation; and **Kisiel *et al*.** (2025) revealed local strain inhomogeneities at the nanoscale that pin or guide the transition front during electrical triggering. The resistance drops abruptly, mimicking a neuronal spike. When the pulse ends, the material cools and recovers its insulating state. By controlling device geometry and bias parameters, the threshold voltage, recovery time, and subthreshold integration dynamics can be independently engineered.

Early work by **Ramírez *et al*.** (2009) using first-order reversal curve (FORC) measurements revealed the existence of persistent metallic domains within nominally insulating VO_2 films—an early indication of the rich phase coexistence that underlies neuromorphic behavior. **Sharoni**, **Ramírez**, and **Schuller** (2008) subsequently demonstrated that the MIT in nanoscale VO_2 junctions progresses through a series of discrete avalanches, each corresponding to the switching of a single metallic domain (**Qazilbash *et al*.**, 2007)—a direct physical analog of a neuronal spike (see Fig. 2). **Zimmers *et al*.** (2013) and **Valmianski *et al*.** (2018) then developed quantitative frameworks showing that both Joule heating and direct electric-field effects contribute to the current-induced MIT, with their relative importance depending on device size and operating temperature. This thermal-versus-electronic deconvolution is crucial to engineer devices where one mechanism dominates: thermal switching for robust volatile memory retention, field-driven switching for ultra-low-power operation. Recent studies have further investigated switching speed limits in electrically driven VO_2 devices (**Pofelski *et al*.**, 2026; **Ramírez**, 2026) and reported evidence for a purely electronic insulator-metal transition in rutile VO_2 (**Cheng *et al*.**, 2025); the relative contributions of Mott and Peierls mechanisms remain an open question in the field.

Vanadium sesquioxide (V_2O_3): canonical Mott material

While VO_2 is dominated by combined Mott and Peierls physics, its cousin V_2O_3 (vanadium sesquioxide) undergoes a more "textbook" Mott transition near 160 K in bulk, driven predominantly by electron-electron correlations (**Imada**, **Fujimori**, & **Tokura**, 1998). Epitaxial strain in thin films can shift this temperature upward by 10–20 K. Although the low transition temperature limits direct room-temperature applications, V_2O_3 is a valuable model system for studying pure Mott physics. Its extreme sensitivity to strain and pressure—small perturbations can shift the MIT temperature by tens of kelvin—makes it a platform for strain-engineered neuromorphic devices, and its electrical breakdown behavior (**Guénon *et al*.**, 2013) showcases the sharp, high-contrast switching useful for neuristor implementations.

Niobium dioxide (NbO_2): high-temperature Mott oscillator

Niobium dioxide (NbO_2) is the second major Mott-switch material for neuromorphic applications and complements VO_2 in important ways. Its rutile-structure MIT occurs near 1070 K—far above room temperature—so the insulating state is stable under ambient conditions and the switch is triggered exclusively by local Joule heating: a current pulse heats the device channel above the transition, creating a conductive filament that collapses once the pulse ends. This purely thermal mechanism makes NbO_2 intrinsically volatile, ideal for neuristor oscillators.

The neuromorphic potential of NbO_2 was established by **Pickett**, **Medeiros-Ribeiro**, and **Williams** (2013), who demonstrated a scalable two-terminal neuristor by coupling an NbO_2 Mott memristor with a VO_2 switch in a single stack. The device reproduced leaky-integrate-and-fire dynamics and subthreshold summation, providing the first lithographically scalable Mott neuristor. **Kumar *et al*.** (2014) subsequently showed that networks of such NbO_2-based relaxation oscillators can be synchronized through resistive coupling, demonstrating oscillation frequencies from kilohertz to megahertz at microwatt power levels—the key benchmark for ultra-low-power edge-AI inference. The high MIT

temperature of NbO_2 also confers robustness: the insulating state is not disturbed by moderate ambient heating, and the large thermal margin between room temperature and T_{MIT} makes the threshold voltage relatively insensitive to environmental fluctuations.

Perovskite manganites: multi-state memory through phase separation

The perovskite manganites, with the general formula (La,Pr,Ca)MnO_3 (LPCMO), represent a richer and more complex material platform. These materials exhibit *colossal magnetoresistance* arising from *electronic phase separation*: nanoscopic to mesoscopic domains of ferromagnetic metal coexist with antiferromagnetic charge-ordered insulator, and the relative fraction of each phase determines the macroscopic conductivity (**Dagotto**, **Hotta**, & **Moreo**, 2001).

For neuromorphic applications, the key insight is that the relative volume of metallic versus insulating phases can be precisely controlled by electrical pulses: varying the amplitude and duration of a current pulse controls the local heating and subsequent cooling rate, nucleating different fractions of insulating phase. This allows the device to be set to a continuum of resistance states—analog synaptic weight modulation that is extremely difficult to achieve with conventional binary switches. Moreover, the same device can exhibit both volatile switching (negative differential resistance) and non-volatile multi-state memory, potentially emulating both neuron and synapse in a single material (**Carranza-Celis *et al***., 2025).

Table 1 summarizes the four material systems discussed above along the properties most relevant for device design.

Table 1. Comparison of Mott material systems for neuromorphic devices. T_{MIT} values are for unstrained bulk/film samples; strain and doping shift these substantially (see text). "n.r.": not systematically reported in the studies cited above.

Material	T_{MIT}	Mechanism	Volatile / non-volatile	ΔR	Function	Advantages	Limitations	Refs.
VO_2	∼340 K	Mott–Peierls (hybrid)	Volatile (threshold); non-volatile via H-doping	$\sim 10^4$	Neuristor	Near-RT; sharp, fast switching; mature growth	Joule-heating crosstalk; CMOS-incompatible growth	(**Goodenough**, 1971; **Valmianski *et al***., 2018)
V_2O_3	∼160 K (bulk)	Mott (canonical)	Volatile; multi-state via MIT Fingerprinting	n.r.	Neuristor; model system	Strain/pressure tunable; benchmark Mott physics	Sub-room-temperature operation	(**Guénon *et al***., 2013; **Imada**, **Fujimori**, & **Tokura**, 1998)
NbO_2	∼1070 K	Thermal (Joule-driven)	Volatile only	n.r.	Neuristor oscillator	High-T stability; μW oscillators; scalable	No non-volatile/synaptic state	(**Kumar *et al***., 2014; **Pickett**, **Medeiros-Ribeiro**, & **Williams**, 2013)
LPCMO	Broad (phase separation, no single T_c)	Electronic phase separation	Both volatile (NDR) and non-volatile	$\sim 10^7$	Synaptor	Widest demonstrated ΔR; electric/magnetic control	Sub-room-temperature; multi-parameter control	(**Carranza-Celis *et al***., 2025; **Dagotto**, **Hotta**, & **Moreo**, 2001)

Revista de la Academia Colombiana de Ciencias Exactas, Físicas y Naturales. 2026
doi: https://doi.org/10.18257/raccefyn.4169

From Material to Device: Neuromorphic Primitives

To emulate the brain's computational primitives, electronic devices must exhibit either volatile threshold switching (for neurons, or neuristors) or non-volatile resistive switching (for synapses, or synaptors). These two behaviors are distinguished by their current-voltage (I-V) characteristics, as schematically shown in Fig. 3. Volatile threshold switching is characterized by an abrupt drop from the high-resistance state (HRS) to the low-resistance state (LRS) at a threshold voltage (V_{th}), followed by spontaneous recovery to the HRS when the voltage falls below a holding voltage (V_{hold}) (Fig. 3a). In contrast, non-volatile resistive switching preserves multiple stable resistance states at zero bias. Depending on the dominant mechanism, switching can be *bipolar*—requiring set and reset sweeps of opposite polarities (Fig. 3b)—or *unipolar*, where both set and reset occur at the same polarity but at different voltage magnitudes, as in thermally-driven Mott devices such as LPCMO manganites (Fig. 3c).

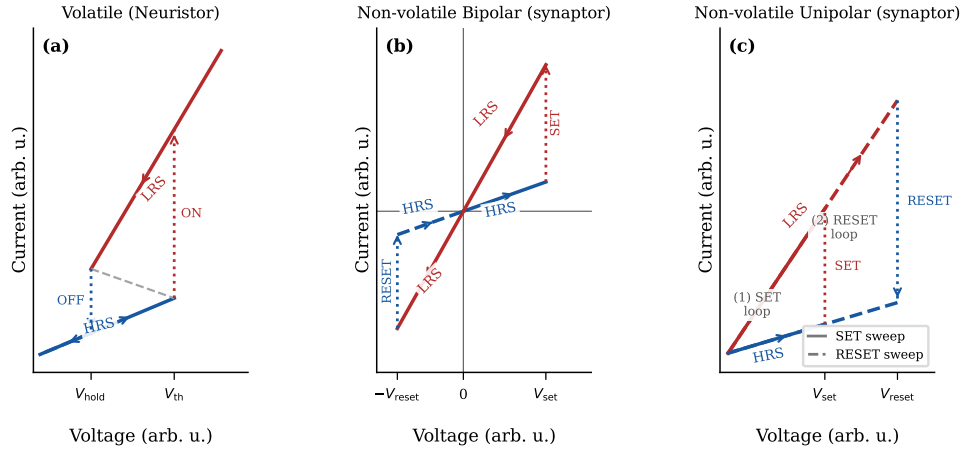

Figure 3. Schematic I-V characteristics of neuromorphic switching primitives. (a) Volatile threshold switching (neuristor): HRS→LRS at V_{th}; spontaneous recovery below V_{hold}. (b) Non-volatile bipolar switching (generic synaptor): set and reset at opposite polarities; both states stable at zero bias. (c) Non-volatile unipolar switching ($V_{\mathrm{reset}} > V_{\mathrm{set}}$, same polarity): the regime of synaptors such as LPCMO manganites.

The neuristor: an artificial neuron

A *neuristor* is a two-terminal device that exhibits LIF neuron behavior through its intrinsic material physics. The concept was introduced by **Crane** (1962), who proposed that nonlinear transmission-line elements could propagate nerve-like pulses; the modern Mott implementation was established by **Pickett**, **Medeiros-Ribeiro**, and **Williams** (2013). In a VO_2 neuristor, a sequence of input current pulses each slightly warms the insulating film. If the inter-pulse interval is shorter than the thermal recovery time, heat accumulates and eventually the local temperature crosses the MIT threshold, producing a resistive collapse—the "spike." If the interval is longer, the material fully recovers and no spike occurs. This cumulative, history-dependent integration is genuine LIF dynamics in a single material device, as demonstrated independently in NbO_2 (**Pickett**, **Medeiros-Ribeiro**, & **Williams**, 2013) and in several other Mott insulators (**Stoliar *et al***., 2017).

A particularly striking result was reported by del **Valle *et al***. (2019): voltage pulses applied just *below* the individual switching threshold could nonetheless trigger switching when applied in rapid succession—"subthreshold firing." This is the hallmark of dendritic computation in biological neurons, where weak but temporally coincident inputs can trigger

a spike even when no single input would individually suffice. The observation of this behavior in a Mott nanodevice (del **Valle *et al***., 2019) demonstrated that the intrinsic physics of phase nucleation and domain growth in Mott materials endows the device with computational capabilities beyond a simple threshold switch, representing a clear demonstration of neuromorphic behavior intrinsic to quantum materials physics. Building on these concepts, recent works have demonstrated energy-efficient Mott activation neurons for full-hardware neural network implementations (**Oh *et al***., 2021) and reconfigurable cascaded thermal neuristors to perform cascading operations in neuristor networks (**Qiu *et al***., 2023).

The synaptor: an artificial synapse

A *synaptor* is a two-terminal Mott-based device whose resistance represents a synaptic weight that can be incrementally modified by electrical pulses and retained non-volatilely. For practical neuromorphic use it must: (1) support multiple stable resistance states; (2) retain those states without applied power; and (3) allow analog, gradual weight updates of arbitrary sign and magnitude.

Phase-separated manganites naturally satisfy all three requirements. By controlling the thermal path followed during resistive switching—the peak temperature reached and the cooling rate applied—different fractions of metallic and insulating domains can be stabilized, yielding non-volatile multi-state resistance. The electrical-pulse amplitude and duration become the “dials” for setting the synaptic weight.

An even more integration-friendly approach is to combine VO_2 and manganite layers within a single bilayer device, encoding both volatile and non-volatile functionality in one stack without additional selector transistors. In $VO_2/La_{0.7}Sr_{0.3}MnO_3$ (LSMO) bilayer memristive devices, both volatile and non-volatile switching modes coexist within a single device structure (**Kunwar *et al***., 2024), as illustrated in Fig. 4. The upper I-V panel shows the abrupt threshold spike characteristic of volatile neuristor operation, while the lower panel shows the gradual, multi-state resistance modulation of the non-volatile synaptor mode. Specifically, the non-volatile mode is driven by the migration of oxygen vacancies at the VO_2/LSMO interface at higher bias voltages, whereas the volatile mode is controlled by the MIT of VO_2 under lower bias voltages. This reconfigurability allows a single device to emulate both neuronal and synaptic functions without requiring additional transistor selectors, pointing to a highly integrated neuromorphic architecture.

Revista de la Academia Colombiana de Ciencias Exactas, Físicas y Naturales. 2026
doi: https://doi.org/10.18257/raccefyn.4169

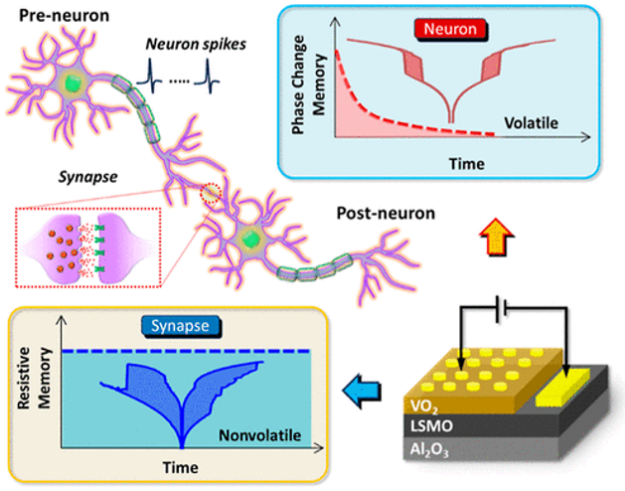

Figure 4. Reconfigurable volatile and non-volatile switching in a single VO_2/LSMO device. Volatile MIT-driven switching (upper right) and non-volatile oxygen-vacancy-driven switching (lower left) coexist in one bilayer stack, enabling a single device to emulate both neuron and synapse. Device schematic at bottom right. Adapted with permission from **Kunwar *et al***. (2024). Copyright 2024 American Chemical Society.

Key Experimental Contributions

The results described in this section span four complementary levels of the neuromorphic stack: direct imaging of the phase-coexistence dynamics that underlie Mott switching, engineering of controllable multi-state devices via the MIT Fingerprinting technique, a demonstration of biologically faithful subthreshold firing in a VO_2 nanodevice, and the realization of multi-state analog memory in LPCMO manganites and multiferroic oxides. Together, these results trace a coherent path from microscopic Mott physics to device-level neuromorphic functionality.

Visualizing phase coexistence in V_2O_3

Using a cryogenic near-field infrared microscope—a scanning probe capable of mapping local optical (and thus electronic) properties with 25 nm spatial resolution—the collaborating groups directly imaged the real-space evolution of the metal-insulator transition in a strained V_2O_3 thin film (**McLeod *et al***., 2017) whose MIT occurs near 170 K (shifted from the bulk value of $\sim$160 K by epitaxial strain), imaging the transition over the 164–184 K window shown in Fig. 5(b)–(e).

The images revealed a spontaneous nanotexture: insulating and metallic phases coexist not randomly but in an ordered pattern of stripes and droplets (panels (b)–(e) of Fig. 5). At temperatures just above the electronic transition, stripes of the insulating phase nucleate along crystallographic directions guided by structural domain walls from an underlying lattice transition—much as water crystallizes preferentially along cracks on a surface. Further cooling removes this structural guidance, and the texture transforms into isotropic metallic "droplets" surrounded by an insulating sea, driven by long-range Coulomb interactions between charged domains.

For neuromorphic applications, the rich spatial heterogeneity is an asset: the coexisting phases provide a natural landscape of intermediate resistance states accessible without external engineering.

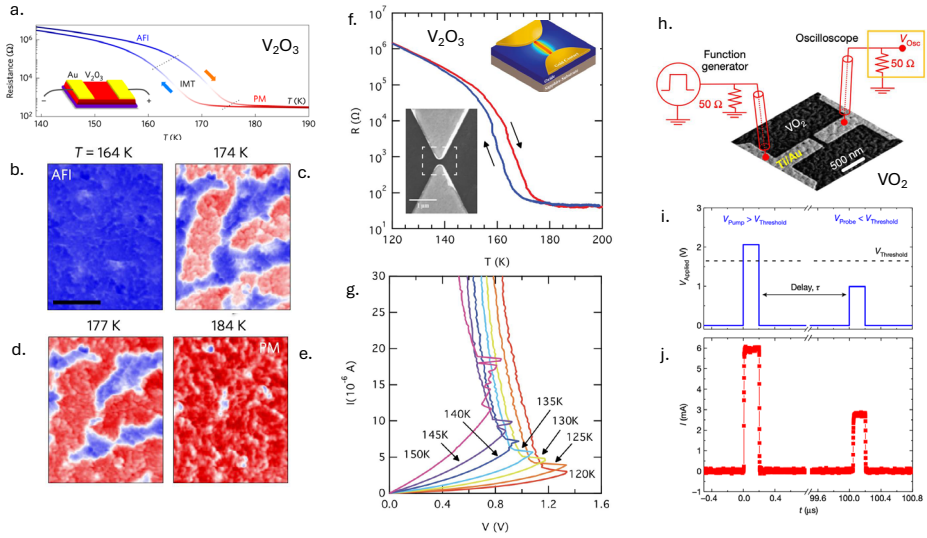

Figure 5. Key experimental contributions in Mott neuromorphic devices. *Left* (**McLeod *et al***., 2017): (a) R-T loop of the V_2O_3 transition from antiferromagnetic insulator (AFI) to paramagnetic metal (PM). (b)–(e) Near-field infrared images at 164, 174, 177, and 184 K revealing nanotextured coexistence of insulating (blue) and metallic (red) domains across the film's MIT. *Center* (**Valmianski *et al***., 2018): (f) R-T hysteresis with COMSOL filament simulation (inset). (g) I-V curves at 120–150 K; threshold shift with temperature enables deconvolution of thermal and field-driven switching. *Right* (del **Valle *et al***., 2019): (h) VO_2 nanodevice and pump-probe circuit. (i) Voltage protocol: above-threshold pump pulse followed by below-threshold probe at delay τ. (j) Current response: probe fires a resistive spike only when τ is short enough that residual heat has not dissipated—subthreshold LIF firing. Left panels adapted with permission from **McLeod *et al***. (2017). Copyright 2017 Springer Nature. Right panels adapted with permission from del **Valle *et al***. (2019). Copyright 2019 Springer Nature.

MIT Fingerprinting: engineering multi-state V_2O_3 devices

A key challenge in V_2O_3 neuromorphic devices is understanding and controlling the mechanisms that drive current-induced resistance switching. Work from the authors' group (**Valmianski *et al***., 2018) used pulsed I-V measurements at multiple temperatures and device geometries—as shown for V_2O_3 in Fig. 5, panels (f)–(g)—to establish that both Joule-heating (thermal) and direct electric-field effects contribute to the current-induced MIT. The result provides clear design rules: nanoscale devices operated near the MIT temperature favor field-driven switching (ultralow power), while larger devices relying on Joule heating offer more predictable, temperature-robust operation.

Building on this insight, the authors' group developed the "MIT Fingerprinting" technique (**Ramírez**, 2026), described in detail in a companion article in this journal. This technique uses pulsed current-voltage (I-V) curves across a wide temperature range and computes the switching derivative $\mathrm{d}V/\mathrm{d}I$ to decompose the switching landscape into distinct electronic and thermal branches. This fingerprint transforms device characterization from qualitative observation into a quantitative engineering tool, showing that device miniaturization expands the accessible multi-state landscape for rational design of analog neuromorphic synaptors.

Subthreshold firing in Mott nanodevices

When a VO_2 nanodevice ($\lesssim 1\,\mu$m gap) is subjected to a train of current pulses each just below the individual switching threshold, the device fires a resistive spike after a sufficient number of pulses (del **Valle *et al***., 2019)—subthreshold integration and firing identical to what biological neurons achieve through dendritic summation.

Revista de la Academia Colombiana de Ciencias Exactas, Físicas y Naturales. 2026
doi: https://doi.org/10.18257/raccefyn.4169

Crucially, the number of pulses required to fire depends on the inter-pulse interval: rapid pulses accumulate heat (or injected carriers) faster than the recovery time allows dissipation, so fewer pulses are needed. Slow pulses allow full recovery between inputs, so they cannot trigger firing regardless of how many are applied. This temporal selectivity is not programmed in; it emerges directly from the Mott physics of phase nucleation, thermal diffusion, and domain dynamics. The result establishes that Mott materials can compute using their own physics, not merely approximate computation through circuits. The individual firing event is probabilistic, but the firing probability as a function of pulse count and inter-pulse interval is reproducible and follows a well-defined statistical trend across repeated measurements on the same device (del **Valle** ***et al***., 2019): the underlying stochasticity, rooted in intrinsic disorder and the local distribution of critical temperatures across grains, is therefore physically consistent rather than uncontrolled variability (see *Device variability* in Challenges and Future Directions).

Multi-state switching in manganites and multiferroic oxides

Recent work from the authors' group on $La_{5/8-x}Pr_xCa_{3/8}MnO_3$ (LPCMO) thin films demonstrated multi-modal analog switching and investigated the phase separation dynamics using ferromagnetic resonance (**Carranza-Celis** ***et al***., 2021; **Carranza-Celis** ***et al***., 2025; **Gomide** ***et al***., 2025). Short electrical pulses drive local heating, quenching the material into configurations with specific metallic-to-insulating phase ratios. Importantly, an applied magnetic field provides an independent control knob: the metamagnetic transition in LPCMO converts insulating domains into ferromagnetic metallic ones, allowing fine-tuning of resistance toward lower values independent of the electrical history. In the most advanced demonstrations, non-volatile multilevel resistance states spanning approximately six orders of magnitude have been achieved in a single LPCMO device (**Carranza-Celis** ***et al***., 2025), enabling analog synaptic operation comparable to what deep-learning inference requires. This combined electric-and-magnetic control is unique to phase-separated manganites and opens avenues for neuromorphic devices that integrate information from both electrical and magnetic stimuli simultaneously.

The collaborating groups have further investigated resistive switching in multiferroic $BiFeO_3$ (BFO) devices (**Cardona-Rodríguez** ***et al***., 2019; **Ceballos Medina** ***et al***., 2025). In early work on BFO/Nb:STO capacitor structures, it was shown that two mechanisms contribute to resistive switching: ferroelectric polarization reversal dominates near the coercive voltage, while oxygen vacancy migration takes over at higher applied voltages—establishing that the BFO switching response is sensitive to both voltage amplitude and polarization history (**Cardona-Rodríguez** ***et al***., 2019). Subsequent studies found that electrode choice dramatically amplifies this effect: devices with silver (Ag) electrodes achieve resistance ratios approximately three times larger than those with YBCO electrodes, because Ag participates in electrochemical filament formation alongside Poole-Frenkel conduction (**Ceballos Medina** ***et al***., 2025). Separately, BFO nanoparticles synthesized by the authors' group (**Carranza-Celis** ***et al***., 2019) show size-tunable multiferroic properties—coexistent ferroelectricity and ferromagnetism at room temperature whose relative strengths can be dialed by controlling particle size—providing another knob for engineering oxide-based neuromorphic devices.

Applications and Demonstrations

The neuristor and synaptor primitives introduced above open access to a broad range of application domains, summarized schematically in Fig. 6 and described in the following subsections.

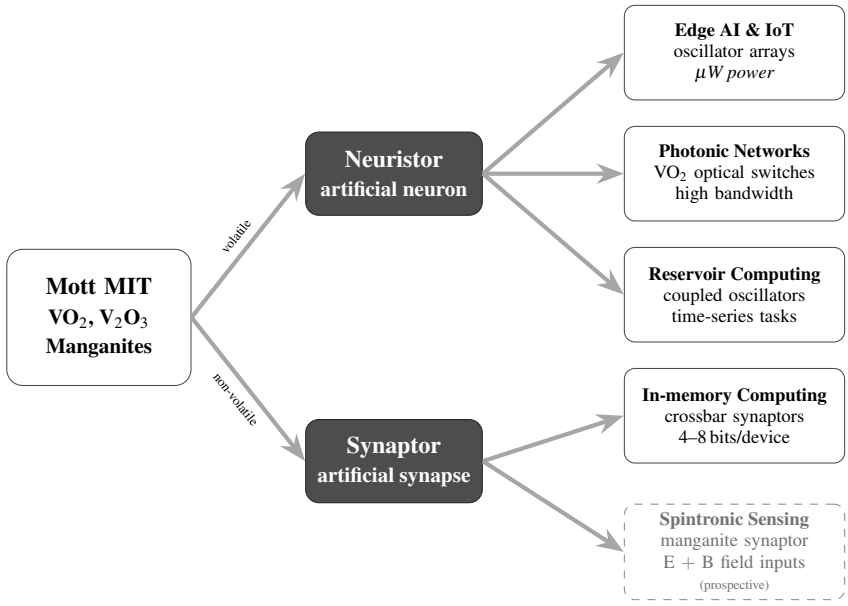

Figure 6. Application landscape of Mott neuromorphic hardware. The *neuristor* (volatile) and *synaptor* (non-volatile) primitives enable three demonstrated application domains discussed in this section: edge-AI oscillator networks, in-memory crossbar inference, and physical reservoir computing. Photonic and magnetic sensing directions are discussed as emerging opportunities in the Challenges and Future Directions section.

Edge AI, in-memory inference, and the Internet of Things

One of the most pressing near-term applications for neuromorphic hardware is *edge AI*: AI inference directly on low-power devices—sensors, wearables, industrial monitors—without sending data to a remote server. These applications demand power in the milliwatt range, far below the kilowatts consumed by GPU-based data centers, and they require both a compute element and a memory element—precisely what the neuristor and synaptor provide.

On the compute side, neuristor oscillators based on NbO_2 and VO_2 have demonstrated oscillation frequencies from kilohertz to megahertz with power consumption in the microwatt range (**Kumar *et al*.**, 2014; **Pickett**, **Medeiros-Ribeiro**, & **Williams**, 2013)—four to five orders of magnitude more efficient than a GPU core. An array of coupled neuristor oscillators can implement pattern recognition through *synchronization*: inputs matching a stored pattern induce coherent oscillation, while mismatched inputs produce incoherent dynamics, making this paradigm naturally suited to always-on applications such as keyword spotting, gesture recognition, or anomaly detection.

On the memory side, a crossbar array of synaptor devices—one at each row-column intersection—implements matrix-vector multiplication *in place*, directly eliminating the von Neumann bottleneck for neural network inference. Multi-state synaptors can store 4–8 bits of weight precision per device rather than the single bit of a binary memristor, dramatically increasing information density. The MIT Fingerprinting approach provides a rational framework for designing the number and spacing of accessible states to match the precision requirements of a target network architecture.

Reservoir computing with Mott oscillator networks

A compelling and relatively recent application of Mott materials is *reservoir computing* (RC)—a paradigm particularly well suited to processing time-varying signals such as speech, vibration, or sensor streams (**Seoane**, 2019; **Tanaka *et al*.**, 2019). See Fig. 7. In

Revista de la Academia Colombiana de Ciencias Exactas, Físicas y Naturales. 2026
doi: https://doi.org/10.18257/raccefyn.4169

conventional recurrent neural networks, all synaptic connections must be trained, which is computationally expensive. RC bypasses this by using a fixed, complex dynamical system—the "reservoir"—to map inputs into a high-dimensional state space, and training only a simple linear output layer to read out those states. Because the reservoir itself is never optimized, it does not need to be simulated in software: it can be replaced by a physical dynamical system, opening the door to "material-native" computation.

The key requirements for a good physical reservoir are: (i) nonlinearity, to separate inputs that would otherwise look similar; (ii) high dimensionality, so that many independent state variables are available to the readout; and (iii) *fading memory*—recent inputs should influence the current state more than distant ones, while old inputs are gradually forgotten. Networks of coupled VO_2 oscillators satisfy all three naturally. Each oscillator is a nonlinear relaxation element; when coupled, an array of N oscillators produces an N-dimensional dynamical trajectory; and the thermal relaxation time of each Mott switch provides the fading memory time scale. Input signals are injected by modulating the bias current of one or more oscillators, and the instantaneous voltages of all oscillators form the reservoir state vector, which a trained linear layer classifies offline.

Recent experimental work has validated this approach with VO_2. **Corti *et al***. (2018) demonstrated pattern recognition using compact networks of resistively coupled VO_2 oscillators, providing an early proof-of-concept for synchronization-based computing in Mott materials. This was extended by **Corti *et al***. (2021), who showed that coupled VO_2 oscillator circuits can function as analog preprocessing layers for convolutional neural networks, converting image inputs into synchronized phase-delay signals and reducing the computational load on subsequent digital stages. Phase-encoded logic implementations of oscillatory neural networks have further confirmed that VO_2 transition dynamics can natively execute pattern recognition without explicit programming (**Núñez *et al***., 2021), while differential oscillator networks have broadened the range of computational tasks addressable by such architectures (**Jiménez *et al***., 2023). Beyond purely electrical oscillators, **Liu *et al***. (2023) demonstrated physical reservoir computing using oxygen-ion dynamics in a Mott oxide channel, showing that ion-mediated state variables in correlated materials provide additional temporal memory depth beyond what thermal relaxation alone offers. Complementing these oscillator-network demonstrations, **Delacour** and **Todri-Sanial** (2021) derived an explicit mapping from Hebbian learning rules to the coupling resistances of oscillatory VO_2 networks (Fig. 7, panels C–F), providing a concrete route toward on-chip unsupervised learning in Mott-based reservoirs. Continuous synaptic weight adaptation has also been demonstrated directly in VO_2 devices: **Deng *et al***. (2023) monolithically integrated a threshold-firing VO_2 neuron and a non-volatile, selectively H-doped VO_2 synapse on the same substrate, with the synaptic resistance state continuously tunable by consecutive positive or negative voltage pulses.

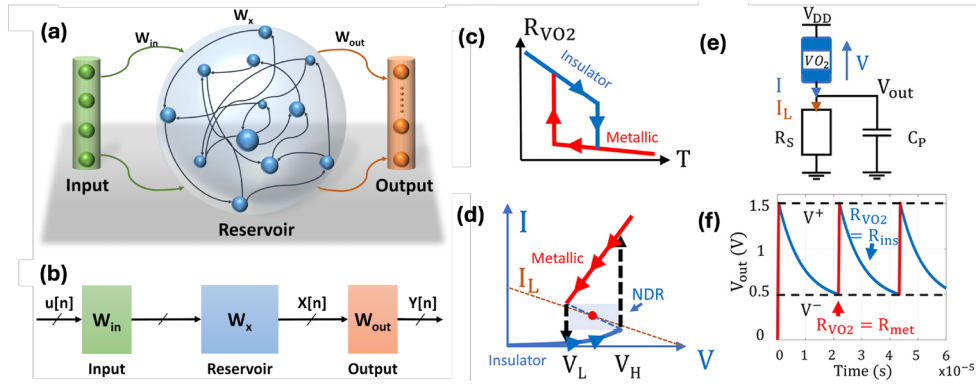

Figure 7. Physical reservoir computing with coupled VO_2 oscillators. (A,B) Echo State Network architecture and block diagram: only W_{out} is trained; the reservoir maps input $u[n]$ to high-dimensional state $X[n]$. Adapted from **Kudithipudi *et al*.** (2016) (CC BY 4.0). (C) VO_2 R-T hysteresis. (D) VO_2 I-V switching at V_H and V_L. (E) Oscillator circuit: VO_2 with load R_S and capacitor C_P. (F) Voltage oscillations at V_{out}; period $\approx 15\,\mu$s. Panels (C–F) adapted from **Delacour** and **Todri-Sanial** (2021) (CC BY 4.0).

The energy cost of Mott-based RC is dominated by the oscillation power of the devices (μW–mW range), making it orders of magnitude more efficient than running an equivalent recurrent neural network on a conventional processor. This positions VO_2 reservoir computing as a promising path toward ultra-low-power, low-latency sensory processing at the edge—for applications such as keyword spotting, gesture recognition, or anomaly detection in industrial sensors—without the need for cloud connectivity or GPU-class hardware.

Challenges and Future Directions

Despite remarkable laboratory progress, significant challenges stand between current demonstrations and practical Mott-based neuromorphic systems.

Device variability. Switching characteristics of Mott devices depend sensitively on local microstructure, grain boundaries, defect distributions, and surface chemistry. Nominally identical devices on the same chip can show significantly different threshold voltages, switching energies, and retention times—a variability far exceeding what CMOS memory tolerates. Interestingly, controlled variability is not necessarily detrimental: neural networks with noisy synaptic weights can outperform their deterministic counterparts on certain tasks through implicit regularization. MIT Fingerprinting can contribute by quantitatively mapping the variability landscape per device rather than reporting only mean values, enabling algorithms to exploit rather than fight the variability. Mitigation strategies developed across the wider resistive-switching community apply directly to Mott oxides: tighter stoichiometric control and electrode engineering reduce the nucleation-site inhomogeneities that drive device-to-device spread (del **Valle *et al*.**, 2018), while epitaxial strain optimization can homogenize the local transition temperature across a film (**Ramírez *et al*.**, 2009). These approaches are complementary to, not a substitute for, statistical per-device characterization.

CMOS integration. High-quality correlated oxide films typically require growth at 650–800°C in controlled oxygen atmospheres, incompatible with standard back-end-of-line CMOS processing (del **Valle *et al*.**, 2018). Low-temperature synthesis routes including atomic layer deposition, and the use of van der Waals 2D materials as strain-relieving buffer layers, are among the most promising strategies to narrow this compatibility gap.

Thermal management. Mott switching is inherently thermal: the same Joule heating that enables low-power switching can cause crosstalk between neighboring devices in

Revista de la Academia Colombiana de Ciencias Exactas, Físicas y Naturales. 2026
doi: https://doi.org/10.18257/raccefyn.4169

integrated networks, disrupting synchronization dynamics and degrading device isolation (**Torres**, **Basaran**, & **Schuller**, 2023). Substrate thermal conductivity, device geometry, and duty-cycle engineering are key variables for mitigating these effects in scaled oscillator arrays.

Endurance and reliability. Biological synapses withstand millions of plasticity cycles without degradation. Current Mott-based synaptors typically demonstrate endurance of 10^6–10^9 switching cycles before significant drift—adequate for some applications but short of the 10^{12} cycles of the best hafnium-oxide memristors. Understanding and mitigating the microscopic mechanisms of resistance drift (oxygen vacancy redistribution, grain boundary migration, electrode reactions) is essential, and electrode optimization—as demonstrated for BFO devices by **Ceballos Medina *et al***. (2025)—is one available lever.

Positioning against competing technologies. Relative to filamentary RRAM, phase-change memory, FeFET, and ECRAM, Mott devices offer three distinct advantages: intrinsic volatile threshold switching for selector-free LIF neuron emulation; multi-stimulus programmability via electrical and magnetic control in LPCMO; and natural fading memory from thermal relaxation, directly suited to reservoir computing. Their principal disadvantages are sub-room-temperature operation for V_2O_3 and manganites, CMOS growth incompatibility, and endurance below the HfO_x benchmark— trade-offs that define a competitive niche in ultra-low-power edge oscillators, physical reservoir computing, and multi-state analog synapses with magnetic tunability. Representative benchmarks illustrate this trade-off space: optimized RRAM and PCM cells combine 10–100 ns write access times, 10^3–10^7 Ω resistance windows, and 10^6–10^9-cycle endurance (**Sebastian *et al***., 2020), comparable to or better than the pJ-scale switching energies estimated below for Mott neuristors. FeFETs switch on similarly fast timescales but their endurance is typically several orders of magnitude lower than the best RRAM/PCM cells, limited by gate-oxide degradation un-der repeated high-field cycling, while ECRAM trades a less area-scalable three-terminal architecture for high write linearity and endurance advantageous for analog on-chip train-ing. Mott devices are not positioned to outperform these established metrics outright; their niche is the intrinsic threshold and multi-state functionality that RRAM, PCM, FeFET, and ECRAM require additional selector or peripheral circuitry to emulate.

Quantitative energy comparison. Pulsed I–V measurements on VO_2 neuristors (del **Valle *et al***., 2019) show switching triggered by a 1.70 V, 200 ns pulse reaching ∼5 mA; combined with the 1–10 ns intrinsic insulator-to-metal switching time obtained from time-dependent COMSOL simulations in the same study, this yields a switching energy of order $E \approx VI\Delta t \approx$ 10–100 pJ per event, comparable to the sub-pJ-to-tens-of-pJ write energies reported for optimized RRAM and PCM cells. Independent optical pump–probe measurements on VO_2 films give a structural switching time of only 29–80 ps (**Wang *et al***., 2017), a lower bound consistent with this estimate. Steady-state breakdown power in nanoscale VO_2 and V_2O_3 devices (140×200 nm electrode gaps) is only 50–80 µW and 5–9 µW, respectively (**Valmianski *et al***., 2018), pointing to further headroom for energy reduction through device miniaturization.

Approaching room-temperature operation. A known route to raise the V_2O_3 transition temperature toward room temperature is chemical substitution with Cr on the V site, which expands the paramagnetic insulating phase to higher temperatures in the pressure-temperature phase diagram (**Imada**, **Fujimori**, & **Tokura**, 1998). Whether the underlying Mott-Hubbard correlation mechanism survives such heavy chemical doping, or the system crosses over into a disorder-dominated regime, remains an open question that has not been systematically addressed.

Emerging opportunities: photonic and magnetic sensing. The same MIT that enables electrical switching in Mott devices also couples to optical and magnetic degrees of freedom, opening niches inaccessible to conventional electronics. VO_2-based

optical switches integrated into silicon photonics platforms exploit the large change in refractive index across the MIT for all-optical or electro-optical modulation at low energy cost (**Joushaghani *et al*.**, 2014), pointing toward neuromorphic networks that combine light-speed signal propagation with Mott-efficient switching—a potential route to high-bandwidth, ultra-low-power signal processing in telecommunications. On the magnetic side, phase-separated manganites offer a prospective niche that purely electronic materials cannot fill: a synaptor whose resistance responds to both electrical pulses and an applied magnetic field (**Gomide *et al*.**, 2025) could learn to distinguish field-sequence patterns without external processing, with applications in medical imaging, geophysical sensing, or support electronics for quantum computing systems.

Conclusions

Neuromorphic computing with strongly correlated electron materials represents one of the most exciting intersections of quantum condensed matter physics and applied computing. The unique properties of Mott insulators—their dramatic, tunable metal-insulator transitions, their intrinsic multi-state phase coexistence, and their sensitivity to multiple external stimuli—make them natural candidates for implementing the nonlinear, adaptive, and memory-bearing behaviors that energy-efficient brain-inspired hardware requires.

The body of work reviewed here supports this outlook. We can now directly visualize the nanoscale phase coexistence underlying the Mott transition in V_2O_3, systematically map and engineer the multi-state switching landscape in VO_2 devices, demonstrate neuron-like subthreshold firing in Mott nanodevices, and achieve controllable analog synaptic behavior in phase-separated manganites. These are not incremental improvements on existing technology: they represent qualitatively new computational capabilities enabled by quantum materials physics.

The road to practical deployment remains long, with device variability, CMOS compatibility, and system-level integration as formidable engineering challenges. Scaling from the isolated device primitives reviewed here to networks trained under continuous synaptic plasticity and Hebbian-type learning rules is a substantial, distinct research program that lies beyond the scope of this review. The trajectory is clear: as materials synthesis improves, as characterization methods like MIT Fingerprinting mature, and as algorithm designers learn to work with the natural physics of Mott switches rather than against it, neuromorphic hardware based on correlated electron materials holds genuine promise to transform energy-efficient AI—enabling the next generation of intelligent edge devices that process information at the power level of a biological brain, not a data center. Realizing that promise hinges on three milestones that mark the transition from laboratory demonstration to deployable technology: large-scale, wafer-level manufacturing of correlated oxide films with reproducible switching characteristics; genuine compatibility with back-end-of-line CMOS processing, so that Mott devices can be co-integrated with conventional logic rather than replace it; and system-level integration, where individual neuristors and synaptors are assembled into networks whose collective dynamics—not just single-device metrics—determine computational performance. Strongly correlated quantum materials will not displace silicon; their opportunity is to extend it, supplying the nonlinear, adaptive, low-power primitives that conventional CMOS structurally cannot.

Acknowledgments

The authors thank the members of the Condensed Matter and Correlated Oxides group at Universidad de los Andes and the Excellence Center for Novel Materials, CENM, at Universidad del Valle for their contributions to the work reviewed here. Financial support from MINCIENCIAS (Colombia) is gratefully acknowledged. The authors acknowledge the support of Universidad de los Andes, the Facultad de Ciencias, and the Vicerrectoría de Inves-

tigación y Creación through project PROPI-01598-24. Research at UCSD was supported as part of the Quantum Materials for Energy Efficient Neuromorphic Computing (Q-MEEN-C), an Energy Frontier Research Center funded by the U.S. Department of Energy, Office of Science, Basic Energy Sciences under Award # DE-SC0019273.

Author Contributions

J.G.R.: Conceptualization, writing—original draft, writing—review & editing. P.P.: Writing—review & editing. M.E.G.: Writing—review & editing. I.K.S.: Writing—review & editing.

Conflict of Interests

The authors declare having no conflict of interests.

References

Attwell, D., Laughlin, S. B. (2001) An energy budget for signaling in the grey matter of the brain. *Journal of Cerebral Blood Flow & Metabolism*, *21*(10), 1133–1145. https://doi.org/10.1097/00004647-200110000-00001

Cao, J., Zhang, X., Cheng, H., Qiu, J., Liu, X., Wang, M., Liu, Q. (2022) Emerging dynamic memristors for neuromorphic reservoir computing. *Nanoscale*, *14*, 289–298. https://doi.org/10.1039/D1NR06680C

Cardona-Rodríguez, A., Arango, I. C., Gomez, M. F., Dominguez, C., Trastoy, J., Urban, C., Sulekar, S., Nino, J. C., Schuller, I. K., Gomez, M. E. (2019) Resistive switching in multiferroic $BiFeO_3$ films: Ferroelectricity versus vacancy migration. *Solid State Communications*, *288*, 38–42. https://doi.org/10.1016/j.ssc.2018.11.005

Carranza-Celis, D., Cardona-Rodríguez, A., Narváez, J., Moscoso-Londoño, O., Muraca, D., Knobel, M., Ornelas-Soto, N., Reiber, A., Ramírez, J. G. (2019) Control of multiferroic properties in $BiFeO_3$ nanoparticles. *Scientific Reports*, *9*, 3182. https://doi.org/10.1038/s41598-019-39517-3

Carranza-Celis, D., Skoropata, E., Biswas, A., Fitzsimmons, M. R., Schuller, I. K., Ramirez, J. G. (2021) Magnetism dynamics driven by phase separation in pr-doped manganite thin films: A ferromagnetic resonance study. *Physical Review Materials*, *5*(12). https://doi.org/10.1103/physrevmaterials.5.124413

Carranza-Celis, D., Salev, P., Basaran, A. C., Schuller, I. K., Ramírez, J. G. (2025) *Electronic and magnetic memory enabled by phase separation* [Manuscript in preparation].

Ceballos Medina, S., Marín Mercado, L., Cardona-Rodríguez, A., Quiñonez Penagos, M. F., Magén, C., Rodríguez, L. A., Ramírez, J. G. (2025) Resistive switching mechanisms in $BiFeO_3$ devices with YBCO and Ag as top electrodes. *Physics Open*, *22*, 100249. https://doi.org/10.1016/j.physo.2024.100249

Cheng, S., Navarro, H., Wang, Z., Li, X., Kaur, J., Pofelski, A., Meng, Q., Zhou, C., Chen, C., Dean, M. P. M., Liu, M., Basaran, A. C., Rozenberg, M., Ong, S. P., Schuller, I. K., & Zhu, Y. (2025) Purely electronic insulator-metal transition in rutile vo2. *Nature Communications*, *16,* 5444. https://doi.org/10.1038/s41467-025-6 0243-0

Corti, E., Cornejo Jimenez, J. A., Niang, K. M., Robertson, J., Moselund, K. E., Gotsmann, B., Ionescu, A. M., Karg, S. (2021) Coupled VO_2 oscillators circuit as analog first layer filter in convolutional neural networks. *Frontiers in Neuroscience*, *15*, 628254. https://doi.org/10.3389/fnins.2021.628254

Corti, E., Gotsmann, B., Moselund, K., Stolichnov, I., Ionescu, A., Karg, S. (2018) Resistive coupled VO_2 oscillators for image recognition. *2018 IEEE International*

Conference on Rebooting Computing (ICRC), 1–7. https://doi.org/10.1109/icrc.2018.8638626

Crane, H. D. (1962) Neuristor—a novel device and system concept. *Proceedings of the IRE*, *50*(10), 2048–2060. https://doi.org/10.1109/JRPROC.1962.288130

Dagotto, E., Hotta, T., Moreo, A. (2001) Colossal magnetoresistant materials: The key role of phase separation. *Physics Reports*, *344*(1–3), 1–153. https://doi.org/10.1016/S0370-1573(00)00121-6

Davies, M., Srinivasa, N., Lin, T.-H., Chinya, G., Cao, Y., Choday, S. H., Dimou, G., Joshi, P., Imam, N., Jain, S., Liao, Y., Lin, C.-K., Lines, A., Liu, R., Mathaikutty, D., McCoy, S., Paul, A., Tse, J., Venkataramanan, G., … Wang, H. (2018) Loihi: A neuromorphic manycore processor with on-chip learning. *IEEE Micro*, *38*(1), 82–99. https://doi.org/10.1109/MM.2018.112130359

Delacour, C., Todri-Sanial, A. (2021) Mapping Hebbian learning rules to coupling resistances for oscillatory neural networks. *Frontiers in Neuroscience*, *15*, 694549. https://doi.org/10.3389/fnins.2021.694549

del Valle, J., Ramírez, J. G., Rozenberg, M. J., Schuller, I. K. (2018) Challenges in materials and devices for resistive-switching-based neuromorphic computing. *Journal of Applied Physics*, *124*(21), 211101. https://doi.org/10.1063/1.5047800

del Valle, J., Ramírez, J. G., Rozenberg, M. J., Schuller, I. K. (2019) Subthreshold firing in Mott nanodevices. *Nature*, *569*, 388–392. https://doi.org/10.1038/s41586-019-1159-6

del Valle, J., Vargas, N. M., Rocco, R., Salev, P., Kalcheim, Y., Lapa, P. N., Adda, C., Lee, M.-H., Wang, P. Y., Fratino, L., Rozenberg, M. J., Schuller, I. K. (2021) Spatiotemporal characterization of the field-induced insulator-to-metal transition. *Science*, *373*(6557), 907–911. https://doi.org/10.1126/science.abd9088

Deng, S., Yu, H., Park, T. J., Islam, A. N. M. N., Manna, S., Pofelski, A., Wang, Q., Zhu, Y., Sankaranarayanan, S. K. R. S., Sengupta, A., Ramanathan, S. (2023) Selective area doping for Mott neuromorphic electronics. *Science Advances*, *9*(11), eade4838. https://doi.org/10.1126/sciadv.ade4838

Gomide, G. B., Carranza-Celis, D., Kuhl, G., Knobel, M., Ramírez, J. G., Muraca, D. (2025) Voltage-tunable spin resonance in quantum phase-separated material. *APL Materials*, *13*(4), 041122. https://doi.org/10.1063/5.0256253

Goodenough, J. B. (1971) The two components of the crystallographic transition in VO_2. *Journal of Solid State Chemistry*, *3*(4), 490–500. https://doi.org/10.1016/0022-4596(71)90091-0

Guénon, S., Scharinger, S., Wang, S., Ramírez, J. G., Koelle, D., Kleiner, R., Schuller, I. K. (2013) Electrical breakdown in a V_2O_3 device at the insulator-to-metal transition. *EPL (Europhysics Letters)*, *101*(5), 57003. https://doi.org/10.1209/0295-5075/101/57003

Herculano-Houzel, S. (2009) The human brain in numbers: A linearly scaled-up primate brain. *Frontiers in Human Neuroscience*, *3*, 31. https://doi.org/10.3389/neuro.09.031.2009

Imada, M., Fujimori, A., Tokura, Y. (1998) Metal-insulator transitions. *Reviews of Modern Physics*, *70*(4), 1039–1263. https://doi.org/10.1103/RevModPhys.70.1039

Jiménez, M., Núñez, J., Shamsi, J., Linares-Barranco, B., Avedillo, M. J. (2023) Experimental demonstration of coupled differential oscillator networks for versatile applications. *Frontiers in Neuroscience*, *17*, 1294954. https://doi.org/10.3389/fnins.2023.1294954

Joushaghani, A., Jeong, J., Paradis, S., Alain, D., Aitchison, J. S., Poon, J. K. S. (2014) Wavelength-size hybrid Si-VO_2 waveguide electroabsorption optical switches and photodetectors. *Optics Express*, *22*(3), 3968–3976. https://doi.org/10.1364/OE.22.003968

Kisiel, E., Salev, P., Poudyal, I., Alspaugh, D. J., Carneiro, F., Qiu, E., Rodolakis, F., Zhang, Z., Shpyrko, O. G., Rozenberg, M., Schuller, I. K., Islam, Z., Frano, A. (2025) High-resolution full-field structural microscopy of the voltage-induced filament formation in vo₂-based neuromorphic devices. *ACS Nano*, *19*(16), 15385–15394. https://doi.org/10.1021/acsnano.4c14696

Kudithipudi, D., Saleh, Q., Merkel, C., Thesing, J., Wysocki, B. (2016) Design and analysis of a neuromemristive reservoir computing architecture for biosignal processing. *Frontiers in Neuroscience*, *9*, 502. https://doi.org/10.3389/fnins.2015.00502

Kumar, S., Strachan, J. P., Pickett, M. D., Bratkovsky, A., Nishi, Y., Williams, R. S. (2014) Synchronized charge oscillations in correlated electron systems. *Scientific Reports*, *4*, 4964. https://doi.org/10.1038/srep04964

Kunwar, S., Cucciniello, N. P., Mazza, A. R., Zhang, D., Santillan, L., Freiman, B., Roy, P., Jia, Q., MacManus-Driscoll, J. L., Wang, H., Nie, W., Chen, A. (2024) Reconfigurable resistive switching in $VO_2/La_{0.7}Sr_{0.3}MnO_3/Al_2O_3$ (0001) memristive devices for neuromorphic computing. *ACS Applied Materials & Interfaces*, *16*(15), 19103–19111. https://doi.org/10.1021/acsami.3c19032

Laad, M. S., Craco, L. (2024) Mott transitions: A brief review. *Advanced Quantum Technologies*, *7*, 2200186. https://doi.org/10.1002/qute.202200186

Lie, S. (2021) Cerebras CS-2: Architecture and performance of a wafer-scale AI accelerator [2.6 trillion transistors, TSMC 7 nm, system power 23 kW]. *IEEE Hot Chips 33 Symposium (HCS)*. https://doi.org/10.1109/HCS52781.2021.9567183

Liu, Z., Zhang, Q., Xie, D., Zhang, M., Li, X., Zhong, H., Li, G., He, M., Shang, D., Wang, C., Gu, L., Yang, G., Jin, K., Ge, C. (2023) Interface-type tunable oxygen ion dynamics for physical reservoir computing. *Nature Communications*, *14*, 6612. https://doi.org/10.1038/s41467-023-42993-x

McLeod, A. S., van Heumen, E., Ramírez, J. G., Wang, S., Saerbeck, T., Guenon, S., Goldflam, M., Anderegg, L., Kelly, P., Mueller, A., Liu, M. K., Schuller, I. K., Basov, D. N. (2017) Nanotextured phase coexistence in the correlated insulator V_2O_3. *Nature Physics*, *13*, 80–86. https://doi.org/10.1038/nphys3882

Mead, C. (1989) *Analog VLSI and neural systems*. Addison-Wesley.

Merolla, P. A., Arthur, J. V., Alvarez-Icaza, R., Cassidy, A. S., Sawada, J., Akopyan, F., Jackson, B. L., Imam, N., Guo, C., Nakamura, Y., Brezzo, B., Vo, I., Esser, S. K., Appuswamy, R., Taba, B., Amir, A., Flickner, M. D., Risk, W. P., Manohar, R., Modha, D. S. (2014) A million spiking-neuron integrated circuit with a scalable communication network and interface. *Science*, *345*(6197), 668–673. https://doi.org/10.1126/science.1254642

Morrison, V. R., Chatelain, R. P., Tiwari, K. L., Hendaoui, A., Bruhács, A., Chaker, M., Siwick, B. J. (2014) A photoinduced metal-like phase of monoclinic VO_2 revealed by ultrafast electron diffraction. *Science*, *346*(6208), 445-448. https://doi .org/10.1126/science.1253779

Núñez, J., Avedillo, M. J., Jiménez, M., Quintana, J. M., Todri-Sanial, A., Corti, E., Karg, S., Linares-Barranco, B. (2021) Oscillatory neural networks using VO_2 based phase encoded logic. *Frontiers in Neuroscience*, *15*, 655823. https://doi.org/10.3389/fnins.2021.655823

Oh, S., Shi, Y., del Valle, J., Salev, P., Lu, Y., Huang, Z., Kalcheim, Y., Schuller, I. K., Kuzum, D. (2021) Energy-efficient mott activation neuron for full-hardware implementation of neural networks. *Nature Nanotechnology*, *16*(6), 680–687. https://doi.org/10.1038/s41565-021-00874-8

Pickett, M. D., Medeiros-Ribeiro, G., Williams, R. S. (2013) A scalable neuristor built with Mott memristors. *Nature Materials*, *12*(2), 114-117. https://doi.org/10.1038/nmat3510

Pofelski, A., Liu, C., Reisbick, S. A., Han, M.-G., Wu, L., Navarro, H., Qiu, E., Wang, T. D., Mousavi M., S. S., Alspaugh, D. J., Rozenberg, M., Ramanathan, S., Schuller, I. K., & Zhu, Y. (2026) Switching speed limits in electrically driven vo2 structural mott–peierls transition. *Nature Communications*, *17, 3139*. https://doi.org /10.1038/s41467-026-69904-0

Qazilbash, M. M., Brehm, M., Chae, B. G., Ho, P. C., Andreev, G. O., Kim, B. J., Yun, S. J., Balatsky, A. V., Maple, M. B., Keilmann, F., Kim, H. T., Basov, D. N. (2007) Mott transition in VO_2 revealed by infrared spectroscopy and nano-imaging. *Science*, *318*(5857), 1750–1753. https://doi.org/10.1126/science.1150124

Qiu, E., Zhang, Y.-H., Ventra, M. D., Schuller, I. K. (2023) Reconfigurable cascaded thermal neuristors for neuromorphic computing. *Advanced Materials*, *36*(6), 2306818. https ://doi.org/10.1002/adma.202306818

Ramírez, J. G., Sharoni, A., Dubi, Y., Gómez, M. E., Schuller, I. K. (2009) First-order reversal curve measurements of the metal-insulator transition in VO_2: Signatures of persistent metallic domains. *Physical Review B*, *79*(23), 235110. https://doi.org /10.1103/PhysRevB.79.235110

Ramírez, J. G. (2026) Experimental deconvolution of electronic and thermal switching mechanisms in the VO_2 Metal-Insulator Transition. *Revista de la Academia Colombiana de Ciencias Exactas, Físicas y Naturales*, *50*(194), 54-68. https://doi .org/10.18257/raccefyn.3273

Salev, P., Kisiel, E., Sasaki, D., Gunn, B., He, W., Feng, M., Li, J., Tamura, N., Poudyal, I., Islam, Z., Takamura, Y., Frano, A., Schuller, I. K. (2024) Local strain inhomogeneities during electrical triggering of a metal–insulator transition revealed by x-ray microscopy. *Proceedings of the National Academy of Sciences*, *121*(34), e2317944121. https://doi.org/10.1073/pnas.2317944121

Sebastian, A., Le Gallo, M., Khaddam-Aljameh, R., Eleftheriou, E. (2020) Memory devices and applications for in-memory computing. *Nature Nanotechnology*, *15*(7), 529–544. https://doi.org/10.1038/s41565-020-0655-z

Seoane, L. F. (2019) Evolutionary aspects of reservoir computing. *Philosophical Transactions of the Royal Society B*, *374*, 20180377. https://doi.org/10.1098/rstb.2018.0377

Sharoni, A., Ramírez, J. G., Schuller, I. K. (2008) Multiple avalanches across the metal-insulator transition of vanadium oxide nanoscaled junctions. *Physical Review Letters*, *101*(2), 026404. https://doi.org/10.1103/PhysRevLett.101.026404

Stoliar, P., Tranchant, J., Corraze, B., Janod, E., Besland, M.-P., Tesler, F., Rozenberg, M., Cario, L. (2017) A leaky-integrate-and-fire neuron analog realized with a Mott insulator. *Advanced Functional Materials*, *27*(11), 1604740. https://doi.org /10.1002/adfm.201604740

Tanaka, G., Yamane, T., Héroux, J. B., Nakane, R., Kanazawa, N., Takeda, S., Numata, H., Nakano, D., Hirose, A. (2019) Recent advances in physical reservoir computing: A review. *Neural Networks*, *115*, 100-123. https://doi.org/10.1016/j.neunet.2019.03.005

Weber, C., O'Regan, D. D., Hine, N. D. M., Payne, M. C., Kotliar, G., & Littlewood, P. B. (2012) Vanadium dioxide: A Peierls-Mott insulator stable against disorder. Physical *Review Letters*, *108*(25), 256402. https://doi.org/10.1103/PhysRevLett.108.256402

Torres, F., Basaran, A. C., Schuller, I. K. (2023) Thermal management in neuromorphic materials, devices, and networks. *Advanced Materials*, *35*(37), 2205098. https://doi.org/10 .1002/adma.202205098

Valmianski, I., Wang, P. Y., Wang, S., Ramírez, J. G., Guénon, S., Schuller, I. K. (2018) Origin of the current-driven breakdown in vanadium oxides: Thermal versus electronic. *Physical Review B*, *98*(19), 195144. https://doi.org/10.1103/PhysRevB.98.195144

Wang, S., Ramírez, J. G., Jeffet, J., Bar-Ad, S., Huppert, D., Schuller, I. K. (2017) Ultrafast photo-induced dynamics across the metal-insulator transition of VO_2. *EPL (Europhysics Letters)*, *118*, 27005. https://doi.org/10.1209/0295-5075/118/27005

Wang, S., Ramírez, J. G., Schuller, I. K. (2015) Avalanches in vanadium sesquioxide nanodevices. *Physical Review B*, *92*, 085150. https://doi.org/10.1103/PhysRevB.92.085150

Zimmers, A., Aigouy, L., Mortier, M., Sharoni, A., Wang, S., West, K. G., Ramírez, J. G., Schuller, I. K. (2013) Role of thermal heating on the voltage induced insulator-metal transition in VO_2. *Physical Review Letters*, *110*(5), 056601. https://doi.org/10.1103/PhysRevLett.110.056601